# FINITE ELEMENT ANALYSIS OF TRAUMATIC BRAIN INJURIES MECHANISMS IN THE RAT

**Baumgartner D., Lamy M., Willinger R.**
**University of Strasbourg – Institute for Fluid and Solid Mechanics – France**
**Choquet P., Goetz C., Constantinesco A.**
**University of Strasbourg – University Hospital – France**
**Davidsson J.**
**Chalmers University of Technology – Sweden**

## ABSTRACT

A finite element model of the rat's head was developed to improve the knowledge on traumatic brain injuries. A parametric study was conducted on the mechanical characteristics of its anatomical components. A correlation was then established between observed injuries on one hand and intracranial stresses on the other. This result is mainly based on experimental well-defined impacts that generate high rotational accelerations of the head in the sagittal plane. This approach shows the power of numerical tools for better understanding of injury mechanisms and thus for design of protection devices against extreme mechanical loadings of the human body.

**Keywords:** Traumatic brain injuries, Small animal, Finite element method

Traumatic brain injuries (TBI) constitute a significant portion of all injuries occurring as a result of automotive, sports and domestic accidents. Since the brain is one of the most vital organs in a great variety of species, TBI are a critical problem worldwide. It is usually associated with blood vessels failure, such as contusion and haemorrhage. Intracranial bleeding often results in a grooving mass of clotting blood that, if not immediately treated, may result in severe secondary damage and death due to increasing intracranial pressure and distortion of the brain. Besides, brain can suffer from diffuse axonal injuries (DAI) with consequences on the general health. Moreover, the bone structure of the head is also often damaged in case of a head trauma and shows fractures.

The mechanisms of such TBI and head injuries in general have not yet been fully established in spite of a great amount of work. So, over the past fifty years, many studies have been performed to improve the understanding of TBI at the organ as well as at the tissue level. Using finite element models (FEM) to identify injury mechanisms and tissue tolerance limits appears usually as a powerful tool in the framework of real world accidents reconstructions. For example, Baumgartner et al. (2004) proposed mechanisms and tolerance limits based on DAI, subdural haematoma and skull fracture. This study relied on a correlation analysis between real world observed injuries as well as calculated mechanical parameters such as brain pressure or Von Mises stress. Nevertheless, complete validation of a FEM is always affected by errors which are not easy to assess. In fact, this is partly linked to the lack of accurate experimental data. Using an animal model can allow to obtain well-defined mechanical loading conditions of the head which can sometimes be poorly mastered in the framework of a human being accident reconstruction. Thus, it can become easy to control the impact on the head very accurately. Moreover, the animal provides, in addition to the boundary conditions, the complete physiological processes in vivo. This is also a powerful asset that argues in favor of using the animal model. Anderson et al. (1999; 2003) for example, achieved some head impacts on more than ten sheep in order to generate DAI and to link these observed injuries to the mechanical loadings of the head. Nevertheless, the internal dynamic response of the brain in such experimental studies is hard to measure in vivo, especially if the species is of small size. In such a case, a FEM of the impacted anatomical segments can prove helpful since it simulates the cranial and intracranial tissues deformations, strains and stresses.

Currently, living small animals are widely used in different labs as TBI models. In many cases, the rat's head is submitted to either linear or angular acceleration.

In terms of linear acceleration, Marmarou, Foda et al. (1994) used weight drop tests to establish a correlation between the head mechanical loading and the observed injuries. They launched 0.450 kg and 0.500 kg masses at 1 m or 2 m height on the head apex region of two groups of rats. The first group counted 54 rats whereas the second one counted 107 rats. In the first group, Marmarou, Foda et al. (1994) tried to generate bone fractures and head injuries, whereas in the second group they hit the rats to investigate the injury mechanisms by pathophysiological analysis. The acceleration sustained by the rats head where analytically evaluated and raised up to 900 g for 2 m height and 630 g for 1 m height. The impact lasted 0.2 ms in both

cases, and the maximal skull deformation was 0.3 mm for the 900 g acceleration. In terms of injuries, they observed convulsion and apnea consecutively to the impact. They also noticed a small increase in the blood pressure as well as bleeding in the subarachnoid space and in the brain white matter. In the same way, Adelson et al. (1996, 2001), achieved some drop tests on 105 young rats heads. They used masses of 0.075 kg, 0.100 kg and 0.125 kg launched from 2 m height. They underlined that 80% of the specimens died for a mass of 0.125 kg. For masses not exceeding 0.100 kg, they observed 15 seconds hyper and 3 minutes hypo tension, apnea, delayed neurological recovering and diffuse oedema in the corpus callosum. Moreover, Kallakuri et al. (2003) used 12 adult rats and impacted their heads with masses from 1 m, 1.5 m and 2 m heights. They observed some DAI in the corpus callosum by histology analysis. These DAI were in the form of beaded axons, retraction balls and vacuole like enlargements. They scaled DAI with the impact energy. Finally, Shafieian et al. (2007) impacted 7 rats through weight drop tests. They tried to study the effect of their impact device on the elastic properties of the rat's head.

Some other research labs submitted the rat's head to angular acceleration with the same goal of causing injuries. To study the effect of high angular acceleration on the rat's head, Xiao-Sheng et al. (2000) imposed a 90 degrees rotation in the coronal plane to it at a mean speed of 801.27 rad/s and a mean acceleration of 204.4 krad/s². The duration of that short rotation was 2 ms. The 21 rats that survived had diffuse subarachnoid haemorrhage around the brain stem and upper cervical cord but no obvious brain contusion. Axonal swelling and bulblike protrusions on the axonal axis were observed in the medulla oblongata, midbrain, upper cervical cord, and corpus callosum between 6 hours and 144 hours post injury. The axonal injuries were most severe in the brainstem and were accompanied by parenchyma bleeding. In the same way, Fijalkowski et al. (2006, 2007) and Ellingson et al. (2005) submitted 41 rats to high angular accelerations up to 368 krad/s² during 2.1 ms in the coronal plane. All specimens experienced transient unconsciousness and mild ventriculomegaly. Injuries were classified as AIS 2, i.e. classical concussion, based on transient unconsciousness, minimal histological abnormalities, and scaled biomechanics. Davidsson et al. (2009) studied also the effect of high angular acceleration on the rat's and global health. They tested 73 rats in the sagittal plane and induced 20° to 25° rotations to their heads. The peak acceleration ranged between 300 and 2,100 krad/s² during 0.4 ms. Bands of β-APP positive axons were seen in the corpus callosum, thalamus and hippocampus and in the border of these regions in most animals exposed to rotational trauma at 1,100 krad/s² or higher. Similarly for the COX-2 marker above 900 krad/s² the numbers of stained cells were large for a number of locations in the cortex and hippocampus region. The S100 serum analysis indicates that blood vessel and glia cell injuries occurred at rotational accelerations above 1,100 krad/s². Two other teams used rabbits to analyse the consequences of rotational acceleration on the brain tissues in general. Such larger animals allow for some measurements in the intracranial space. Gutierrez et al (2001) submitted 13 albinos rabbits' heads to 212 krad/s² angular acceleration during 0.95 ms in the sagittal plane. They observed subdural haemorrhage that developed during the following 3 days. After 8 to 12 days, they noticed cell inflammation. They also underlined that all animals survived consecutively to the trauma in spite of some apparent concussion in the first days after the impact. Moreover, Krave et al. (2005) measured the brain pressure in 12 female rabbits during the impact. They submitted the rabbits head to an angular acceleration ranging between 94.4 krad/s² and 177.9 krad/s² in the sagittal plane. A pressure sequentially recording revealed different typical characteristics. First, positive and negative pressure peaks having short duration – between 1 ms and 2 ms – were observed, followed by a second, large negative peak value with a comparatively long duration, lasting about 10 ms.

Some labs developed a FEM of the rat's head in order to determine either the mechanical behaviour of the brain and the skull or to establish a correlation between the calculated mechanical parameters and observed injuries. Thus, Gefen et al. (2003) applied an indentation both to skull and brain, as well as to the isolated brain so as to evaluate the tissues rigidity. They noticed that the brain of young rats was more rigid than the brain of adult rats whereas the young rat skull was less rigid because of its smaller thickness. They also pointed out that there was no significant difference between in situ and in vitro tests. This last statement could be discussed since a great deal of other studies (Margulies et al. (2004) for example) showed clear differences between such tests. Moreover, such tests should not be compared due the phenomena that are involved and that are different: blood pressure and other physiological processes. Levchakov et al. (2006) continued the study from Gefen et al. (2003) to take into account the influence of the rat's age on the material properties characterisation. They also analysed the strain and stress distribution in the brain. Therefore they developed a FEM that consisted in 30,000 tetrahedral elements. The FEM simulations indicated that for identical cortical displacements, the neonatal brain may be exposed to larger peak stress magnitudes compared with a mature brain due to stiffer tissue properties in the neonate, as well as larger strain magnitudes due to its smaller size. The brain volume subjected to a certain strain level was greater in the neonate brain compared with the adult models for all indentation depths greater than 1 mm. Mao et al. (2006, 2008) built a highly detailed FEM of the rat's head. This model contains 256,000 hexahedral elements of approximately 0.2 mm size. Most of the current anatomical features

are modelled in this FEM with a special attention to the brain. The validation of that tool relies on the dynamical cortical deformations in the framework of controlled head impacts. They showed a possible correlation between the first principal strain and brain contusions. They also underlined that the intracranial pressure was not correlated with brain bleeding. Moreover, the mechanical threshold upon which contusions are predicted will be influenced by the mechanical behaviour that is implemented in the model.

The aim of the current work is to improve knowledge on TBI due to different impact scenarios based on a FEM of the rat's head developed to predict intracranial mechanical response under impact and infer potential TBI mechanisms. A more distant goal will be to transfer these results to the human brain. Such an approach is used because there are well-defined mechanical loading conditions and injuries sustained available for the animal model but not for humans. The FEM of the rat's head presented here contains less elements that the one developed by Mao et al. (2006, 2008). It could therefore be considered as generally less accurate than the model by Mao et al. (2006, 2008). In fact, it is a compromise between the spatial resolution of the mesh and the computation time. Thus, it consists in a pilot study that may lead to the need of a much more detailed model in order to represent some observed phenomena with better accuracy.

## MATERIAL AND METHODS

### INTRODUCTION

A detailed FEM of the rat's head includes the main anatomical features: the cerebrum, the cerebellum, the olfactory bulbs, the brainstem, the brain/skull interface and the skull. Its geometry is based on Micro-CT for bones and magnetic resonance imaging (MRI) for soft tissues data. The mechanical behaviour of its anatomical components relies on values found in literature. An analysis, quoted as reference analysis, is led on the FEM of the rat's head that is described below. It consists in applying an angular acceleration to the rat's head FEM in the sagittal plane at its centre of mass. This acceleration relies on the experimental study made by Davidsson et al. (2009). In this reference analysis, brain pressure and brain Von Mises stress are computed and compared to the observed injuries in order to elucidate potential brain injury mechanisms and thresholds. A parametric study on the viscous elastic behaviour of the cerebral material was led as well as one on the elasticity properties of the brain/skull interface. The greatest benefit of this study will arise from finding brain-level failure properties. A further step will be to use directly the rat data obtained previously in models of the human head.

### THE FINITE ELEMENT MODEL OF THE RAT'S HEAD

#### Introduction

The development of the FEM needed three main stages. The first one was obtaining the geometry of the different anatomical components of the head. Both other development stages consisted in the meshing of the geometry and in the definition of the mechanical behaviour, the boundary conditions and the loading conditions.

#### MRI and Micro-CT acquisition of the rat head

To maintain the subject in homeostatic conditions, it was kept for both modalities in an isolation cell (Minerve, Esternay, France), anesthetized via a mask using isoflurane in air and immobilized with a tooth bar.

MRI dataset was obtained using a resistive magnet delivering a main magnetic field of 0.1 T (Bouhnik, Vélizy-Villacoublay, France). The head of the rat was enclosed in a solenoid coil aimed at radiofrequency pulse generation and MR signal measurement. A SMIS spectrometer (MRRS, Guildford, U.K.) was used for acquisition sequence generation, based upon a T1 weighted 3D sequence. The 3D Fourier Transform reconstruction led to a volume made of cubic voxels of 500 μm x 500 μm x 500 μm.

Micro-CT was performed using an eXplore RS Locus system (GE Healthcare, Waukesha, U.S.A.) with the following parameters:

- 400 views over 360°.
- 3 frames averaging for each view.
- At 80 kV and 450 μA.

Reconstruction of the tomographic data, using a Feldkamp type algorithm of back projection, led to a volume made of cubic voxels of 93 μm x 93 μm x 93 μm.

The MR data were segmented to extract the brain alone and the Micro-CT data were thresholded to select only bones surfaces.

The MRI apparatus used to obtain images of the rat brain is shown in Fig. 1 (a) with the Micro-CT system used to obtain images of the rat skull (b). Fig. 1 (c) also illustrates the experimental setup inside the MR magnet with a close view of the rat's head.

The MRI apparatus consists in:

- A resistive magnet 0.1 T (Bouhnik SAS) (1).
- A SMIS spectrometer.
- An imaging cell that allows keeping the animal in a warmed environment under anaesthesia during imaging procedure (2).
- An electrical supply of the magnet (3).
- An anaesthesia machine (4).
- Warming and temperature control systems for the imaging cell (5).

Moreover, the same imaging cell used in the MRI system is placed on the cradle of the Micro-CT (6). The opened imaging cell shows the solenoid radio frequency coil surrounding the rat's head which is aimed at MR signal measurement (7).

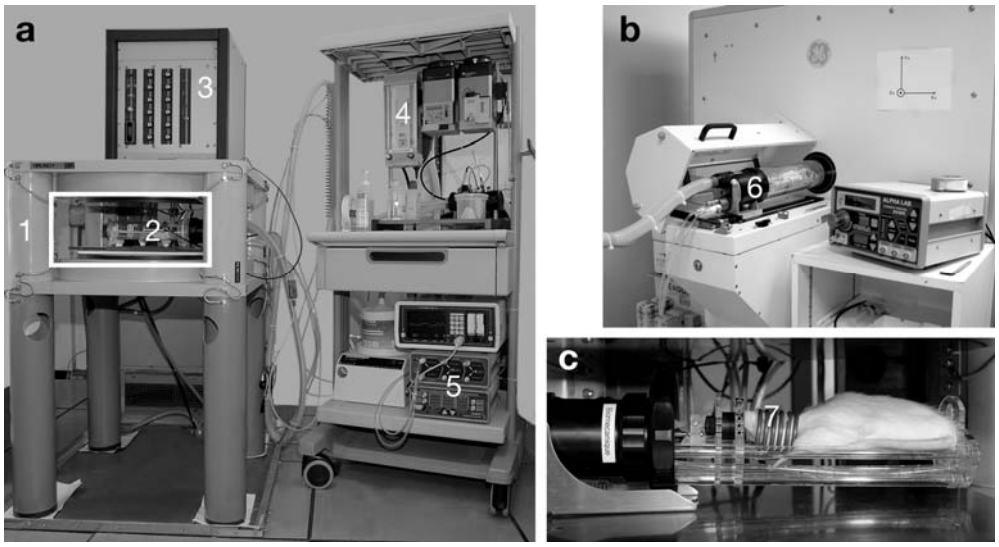


**Fig. 1 – View of the MRI apparatus (a), the Micro-CT system (b) and the experimental setup inside the MR magnet (c).**

Fig. 2 (a) illustrates a view of the MRI complete dataset of the rat's head with the surface encompassing the segmented volume used to build the model. Moreover, the bones are shown in Fig. 2 (b) through their 3D surface rendering of the Micro-CT acquisition. The finite element surface created from the Micro-CT acquisition is shown in Fig. 2 (c).

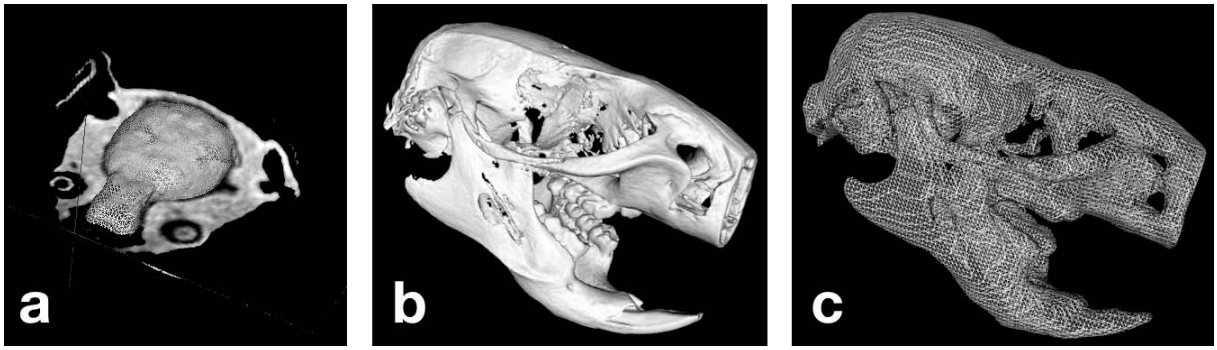


**Fig. 2 –MRI and brain selection (a), surface rendering of the skull from CT data (b) and corresponding mesh (c).**

Meshing of the rat's head

The software used to realise the meshing, based on the data acquired on one Sprague-Dawley rat is ALTAIR HYPERWORKS 9.0 ©. The main anatomical features modelled are the skull (1 layer of shell elements), the brain/skull interface which includes the cerebral spinal fluid and the meninges (1 layer of brick elements), the olfactory bulbs (brick elements), the cerebrum (brick elements), the cerebellum (brick elements)

and the brain stem (brick elements). Fig. 3 shows a cross section of the model and illustrates the anatomical features that are taken into account in that model.

The finite element mesh is continuous and, thus, no numerical interface is necessary. The used types of elements are 4-nodes shell elements and 8-nodes hexahedral elements with a standard Lagrange integration scheme. The average size of the edges of an element is 0.45 mm. The meshing is assumed to be regular in terms of dimension, edge angle and warpage. The skull is simulated with one layer of shell elements with a constant thickness of 0.1 mm whereas the other anatomical components are meshed in hexahedral elements. Overall, the FEM of the rat' head consists in 17,972 hexahedral elements and 3,220 shell elements. Its total mass rises up to 14.1 g.

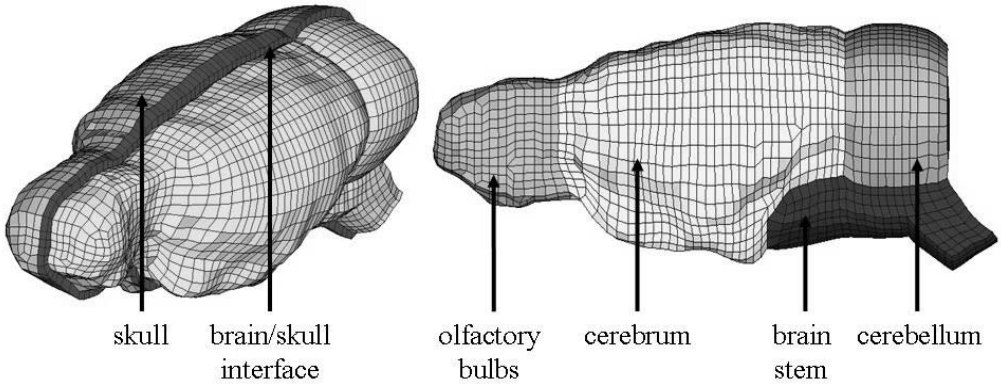


**Fig. 3 – Meshing of the FEM of the rat's head.**

Material properties and boundary conditions

Material characteristics are very important for the success of a FEM. Table 1 lists the properties of the materials used for this FEM of the rat's head. The mechanical behaviour of the skull and of the brain/skull interface is assumed to be linear elastic, isotropic and homogenous. The skull properties are taken from Baumgartner et al. (2004). The brain/skull interface behaviour is inferred from studies from Zhang et al. (2001) and Mao et al. (2006, 2008). Besides, the way of modelling that brain/skull interface is inspired by and copied from previous studies on the human head under trauma from Baumgartner et al. (2004). Indeed, the brain/skull interface was not modeled as a numerical "standard interface" but as a layer of solid elements with an adapted elasticity that allows brain/skull relative motion. Moreover, the olfactory bulbs, the cerebrum, the cerebellum and the brain stem behave as a viscous elastic medium which is also assumed to be isotropic and homogenous. A Boltzman model is adopted for these four parts of the rat's head. The density and the bulk modulus of these anatomical features rely on the study of Zhang et al. (2001) and Mao et al. (2006, 2008). Besides, the short and long term shear moduli are obtained from the work of Gefen et al. (2003). The decay constant of that viscous elastic material is the one proposed by Levchakov et al. (2006).

In each simulation, the head was left free of motion in its 6 degrees of freedom. Thus, it was considered that the neck would not influence the head's dynamical response because of the relative low stiffness of the neck compared to the high amplitude of the head's solicitation.

**Table 1. Material properties of the components of the rat's head FEM**

| | Density [kg/m$^3$] | Young modulus [MPa] | Poisson's ratio | Short term shear modulus [kPa] | Long term shear modulus [kPa] | Bulk modulus [GPa] | Decay constant [s$^{-1}$] |
|---|---|---|---|---|---|---|---|
| Skull | 1800 | 15000 | 0.21 | / | / | / | / |
| Brain/skull interface | 1130 | 20 | 0.45 | / | / | / | / |
| Olfactory bulbs | 1040 | / | / | 1.721 | 0.508 | 2.19 | 0.125 |
| Cerebrum | 1040 | / | / | 1.721 | 0.508 | 2.19 | 0.125 |
| Cerebellum | 1040 | / | / | 1.721 | 0.508 | 2.19 | 0.125 |
| Brain stem | 1040 | / | / | 1.721 | 0.508 | 2.19 | 0.125 |

EXPERIMENTAL IMPACTS ON THE RAT'S HEAD DATA

In brief, 54 male Sprague-Dawley rats weighing 0.415 kg in average were anaesthetized. A midline incision was made through the skin and periosteum on the skull vault. The underlying bone was freed from adherent tissue and a curved plate, denominated skull cap, was secured to the skull by means of dental glue. After a 15 minutes curing period, an attachment plate was fastened by means of two screws to the skull cap, inserted and secured to a rotating bar that can rotate freely around a horizontal axis (Fig. 4). This arrangement gave a brain centre of gravity located about 6.5 mm right above the centre of rotation.

43 of those animals were traumatized i.e. the animal heads were exposed to a short lasting sagittal plane rearward rotational acceleration for about 0.4 ms. This was followed by a rearward rotation at constant velocity and finally the heads came to a stop by a deceleration of about 25% of the initial acceleration (Fig. 5). The rotational acceleration magnitude was varied, by modifying the striker speed, from very low to about 2,000 krad/s². The latter was varied by means of varying the air pressure in a specially designed air driven accelerator. Eleven animals served as sham exposed controls.

To measure rotational acceleration, an Endeveco Isotron 2255B-01 accelerometer was mounted to the rotating bar, was connected to an Endeveco 4416B signal conditioner and its signal was digitized at 200 kHz.

Post-trauma survival times were varied from 2 hours to 5 days. During the scarification of the animals, venous blood was collected to allow for later analysis of the serum. Thereafter, the brains were dissected and either perfusion fixated or fresh frozen. Coronal 14 μm cryostat sections from frontal, central and occipital regions were cut and incubated to study the accumulation of beta-amyloid precursor protein (β-APP) or to assess the presence of cyclooxygenase 2 (COX-2).

In the analysis, two brain sections from each of the three levels in the brain, frontal middle occipital region, were chosen arbitrarily, and β-APP and COX-2 reactivity was assessed by the use of a confocal microscope and white light microscope, respectively. Also, serum S100 levels were assessed with two different immunoassays.

The experimental impacts on rat heads showed an apparent dose-response pattern. The number of β-APP-positive axons increases rapidly at 1,100 krad/s², and for COX-2 intensity the increase starts at around 900 krad/s². The serum analysis supported these findings.

In this rich set of experimental data, the one chosen as reference simulation and to lead the parametric study is the one quoted as N° 27 by Davidsson et al. (2009). It corresponds to a mechanical loading of the rat's head for which soft DAI were diagnosed as well as brain haemorrhages. In fact, for higher levels of angular acceleration, up to 2,000 krad/s², large DAI were observed whereas for lower levels, down to 800 krad/s², no injuries were sustained. Thus, the velocity that is applied to the rat's head in the sagittal plane at its center of mass is illustrated in Fig. 5. That velocity corresponds to an angular acceleration peak of 1,500 krad/s² that is applied during 0.5 ms.

The complete set of numerical simulations (i.e. for the reference analysis as well as for the parametric study) has been realized thanks to the ALTAIR HYPERWORKS 9.0 © software. It consists in a meshing program (HYPERMESH ©), a model preparation program (HYPERCRASH ©), an explicit finite element solver (RADIOSS CRASH ©) and two results exploitation tools (HYPERGRAPH © and HYPERVIEW ©). The simulations ran onto a standard personal computer with and INTEL CENTRINO DUO © processor with 2 GHz of CPU. The simulation of the first 50 ms of each impact lasted one hour approximately. The average time step was beneath $10^{-5}$ ms and the hourglass energy of the model remained under 5% of the total energy thanks to an HEPH element formulation.

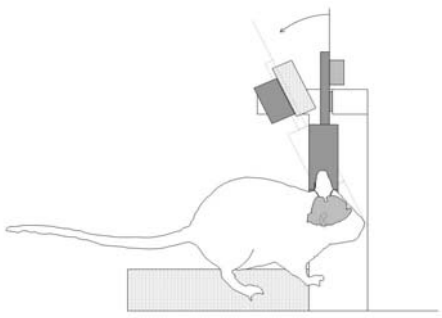

**Fig. 4 – Schematic of the test rig used in the experiments; lateral view.**

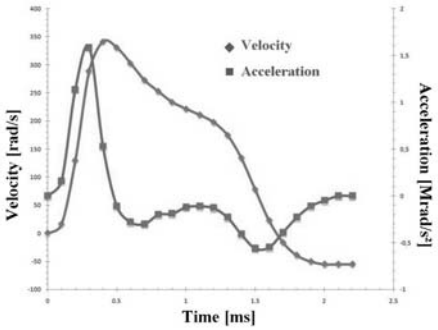


**Fig. 5 – Angular acceleration and velocity that are applied to the rat's head FEM at its centre of mass in the sagittal plane (accelerometer data smoothed using window size 20 rows).**

## RESULTS

### REFERENCE ANALYSIS

In that reference analysis, the FEM of the rat's head used is the one described above. Brain pressure and Von Mises stress are recorded in terms of time history and anatomical distribution in the cerebrum, in the upper and lower part of the olfactory bulbs, in the brain stem and in the cerebellum. Fig 6 illustrates the brain pressure and the brain Von Mises distributions respectively in a sagittal cut view of the brain at the time of their maximal value. Fig. 7 shows the time history of the brain pressure in the lower part of the olfactory bulbs. It must be pointed out that:

- The brain pressure reaches its maximal value 0.3 ms after the beginning of the impact in the lower part of the olfactory bulbs. This value is among 120 kPa.
- The brain Von Mises stress reaches its maximal value 1.4 ms after the beginning of the impact in the upper part of the cerebrum as well as in the corpus callosum. This value is among 0.6 kPa.

One can also note that the brain pressure reaches 72 kPa in the cerebrum, 49 kPa in the upper part of the olfactory bulbs, 69 kPa in the brain stem and 88 kPa in the cerebellum.

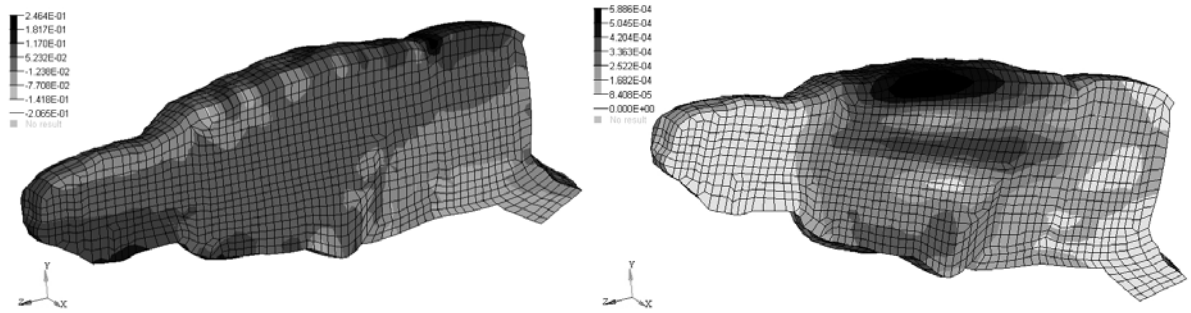


**Fig. 6 – Brain pressure in MPa (left) and Von Mises stress in MPa (right) distribution 0.3 ms and 1.4 ms respectivily after the beginning of the impact.**

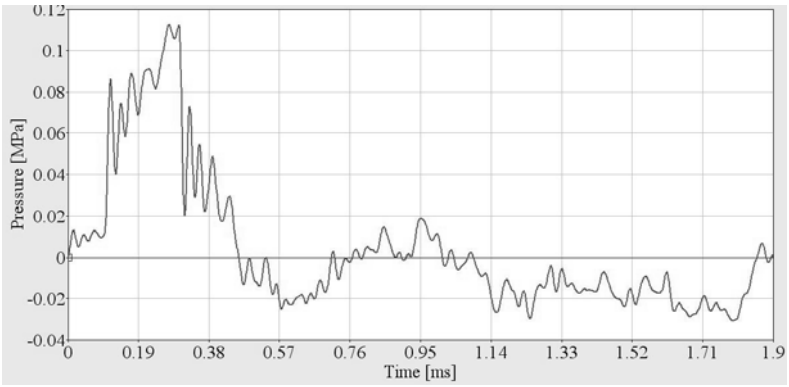


**Fig. 7 – Brain pressure time history in the lower olfactory bulbs.**

### PARAMETRIC ANALYSIS

#### Introduction

Material properties were based on data found in the literature. However, it should be noted that those studies insisted on the fact that precise data concerning the rat brain material behavior are quite sparse. Moreover, depending on the experimental protocol, the values that are acquired for the mechanical behavior of the rat brain can vary greatly. Consequently, numerous simulations were computed, always with the same input measured by Davidsson et al. (2009), illustrated in Fig. 5, but with some changing values for the material properties in terms of short and long term shear moduli, bulk modulus and decay constant of the brain, as well as Young modulus of the brain/skull interface.

Brain short term shear modulus

The brain short term shear modulus varied between 0.17 kPa and 17 kPa while the other mechanical parameters of the model were kept constant at the "reference analysis" level. It took the following values: 0.17 kPa, 0.86 kPa, 1.721 kPa (reference value), 3.44 kPa, 10 kPa and 17 kPa. Whatever the brain area considered, the brain pressure remains constant (112 kPa for its maximum value in the lower part of the olfactory bulbs). Besides, the brain Von Mises stress increases linearly with the brain short term shear modulus as illustrated in Fig. 8 for its maximum value which is reached at the top of the cerebrum 1.4 ms after the beginning of the impact.

Brain long term shear modulus

The brain long term shear modulus varied between 0.05 kPa and 5 kPa while the other mechanical parameters of the model were kept constant at the "reference analysis" level. It took the following values: 0.05 kPa, 0.508 kPa (reference value) and 5 kPa. Whatever the brain area considered, the brain pressure remains constant (112 kPa for its maximum value in the lower part of the olfactory bulbs). Besides, the brain Von Mises stress remains constant (0.59 kPa) with the brain short term long modulus as illustrated in Fig. 9 for its maximum value which is reached at the top of the cerebrum 1.4 ms after the beginning of the impact.

Brain bulk modulus

The brain bulk modulus varied between 0.219 GPa and 21.9 GPa while the other mechanical parameters of the model were kept constant at the "reference analysis" level. It took the following values: 0.219 GPa, 1.125 GPa, 2.19 GPa (reference value), 4.5 GPa and 21.9 GPa. Whatever the brain area considered, the brain pressure remains almost constant with a very slight increase (between 107 kPa and 118 kPa for its maximum value in the lower part of the olfactory bulbs). Besides, the brain Von Mises stress decreases like a power function with the brain bulk modulus as illustrated in Fig. 10 for its maximum value which is reached at the top of the cerebrum 1.4 ms after the beginning of the impact.

Brain decay constant

The brain decay constant varied between 0.00000125 $ms^{-1}$ and 1.25 $ms^{-1}$ while the other mechanical parameters of the model were kept constant at the "reference analysis" level. It took the following different values: 0.00000125 $ms^{-1}$, 0.0000125 $ms^{-1}$, 0.000125 $ms^{-1}$ (reference value), 0.00125 $ms^{-1}$, 0.0125 $ms^{-1}$, 0.125 $ms^{-1}$ and 1.25 $ms^{-1}$. Whatever the brain area considered, the brain pressure remains constant (112 kPa for its maximum value in the lower part of the olfactory bulbs). Besides, the brain Von Mises stress remains constant (0.59 kPa) with the brain decay constant as illustrated in Fig. 11 for its maximum value which is reached at the top of the cerebrum 1.4 ms after the beginning of the impact.

Brain/skull interface Young modulus

The brain/skull interface Young modulus varied between 2 MPa and 200 MPa while the other mechanical parameters of the model were kept constant at the "reference analysis" level. It took the following values: 2 MPa, 10 MPa, 20 MPa (reference value), 100 MPa and 200 MPa. Whatever the brain area considered, the brain pressure remains constant (112 kPa for its maximum value in the lower part of the olfactory bulbs). Besides, the brain Von Mises stress decreases like a power function with the brain/skull interface Young modulus as illustrated in Fig. 12 for its maximum value which is reached at the top of the cerebrum 1.4 ms after the beginning of the impact.

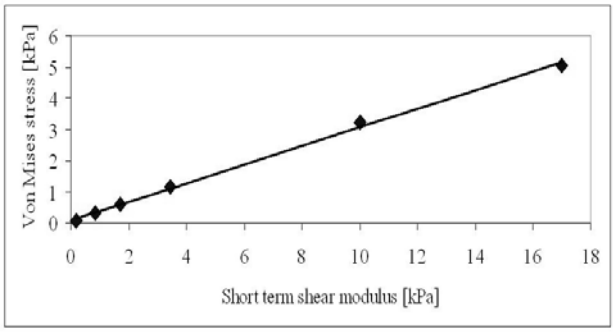


**Fig. 8 – Maximum brain Von Mises stress vs. brain short term shear modulus ($y=0.2982x+0.0819$ – $R^2=0.9977$).**

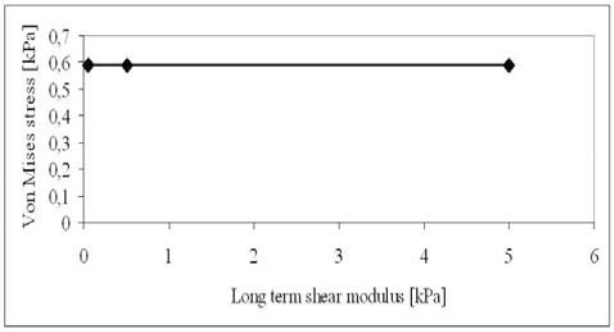


**Fig. 9 – Maximum brain Von Mises stress vs. brain long term shear modulus ($y=0.59$ – $R^2=0.9999$).**

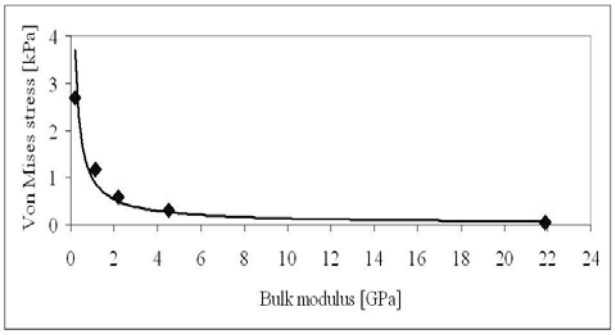


**Fig. 10 – Maximum brain Von Mises stress vs brain bulk modulus ($y=0.9803x^{-0.8743}$ – $R^2=0.9660$).**

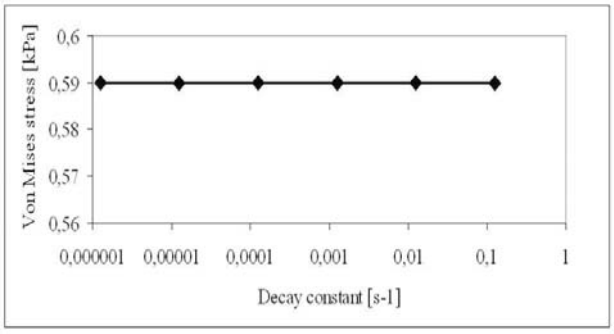


**Fig. 11 – Maximum brain Von Mises stress vs. brain decay constant ($y=0.59$ – $R^2=0.9999$).**

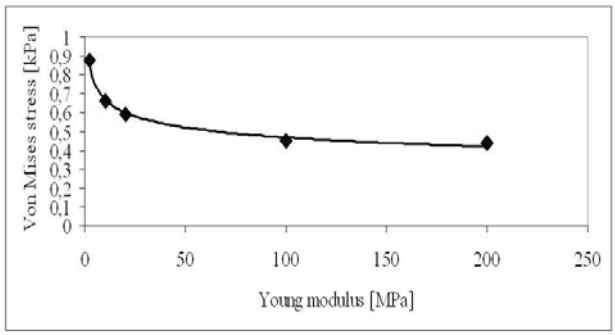


**Fig. 12 – Maximum brain Von Mises stress vs. brain/skull interface Young modulus ($y=0.9571x^{-0.1555}$ – $R^2=0.9857$).**

## DISCUSSION

The parametric analysis of the FEM of the rat's head showed the dependency of the dynamical brain response (consecutively to an external rotational loading) on the three following parameters: the short term shear modulus and the bulk modulus of the brain, as well as the Young modulus of the brain/skull interface. Whereas the brain pressure remains constant with the complete set of mechanical parameters of the model (among 110 kPa in the lower part of the olfactory bulbs), the brain Von Mises stress increases (linearly) with the brain short term shear modulus, and decreases (like a power function) with the brain bulk modulus as well as with the brain/skull interface Young modulus. Thus, these three parameters of the model need particular attention since they vary significantly the dynamic response of the model.

Concerning the comparison between the reference simulation and the experimental results, two different kinds of injuries must be distinguished: focal injuries and diffuse injuries.

As a result of the trauma, haemorrhages could be found in the foramen magnum region, and subdural and subarachnoid haemorrhages were observed on the superior cortex surface in about half of the exposed animals. A few animals suffered from haemorrhages in the vicinity of the olfactory bulb. A limited number of intracranial haemorrhages were noted in some of the animals that had been subjected to rotational accelerations close to 2,000 krad/s². These injuries were also predicted in the reference simulation thanks to the brain pressure. In fact, the correlation between brain pressure and brain haemorrhages was already established by past studies like the one from Ward et al. (1980). They proposed brain pressure as an indicator for brain

haemorrhages upon 200 kPa. The presently calculated value reached 110 kPa in the lower part of the olfactory bulbs which is in the same order of magnitude than the one proposed by Ward et al. (1980). This reinforces the idea that cerebral pressure is a good indicator for focal injuries like brain haemorrhages.

Concerning the diffuse injuries, the trauma caused DAI as indicated by large number of β-APP positive axons, mainly in the vicinity of the corpus callosum as indicated in Fig. 13. The amount of affected axons was more than double in the front region of the brain than in the middle and occipital regions. These injuries were partly well predicted by the reference simulation. In fact, the correlation between brain Von Mises stress and observed DAI or other diffuse neurological injuries was already underlined for sheep (Anderson et al., 1999, 2003) and other animals as well as for human (Baumgartner et al., 2004, Marjoux et al., 2008). The threshold for DAI which was proposed by Marjoux et al. (2008) was around 39 kPa. If the brain Von Mises stress is simulated using the human brain mechanical properties from Baumgartner et al. (2004), the brain Von Mises will reach 40 kPa in different areas of the rat brain under study and especially in the corpus callosum were DAI were observed by Davidsson et al. (2009) Thus, it can be concluded that brain Von Mises appears to be a consolidated indicator for DAI and other brain neurological injuries. Nevertheless, these diffuse injuries were not always well predicted by the brain Von Mises including in some areas like the olfactory bulbs. Possibly the explanation to this is that the stiffness in the rat brain is not uniform and hence local deformation may occur in that front extremity of the rat's brain. Therefore, these injury mechanisms, which rely on brain Von Mises stress or other intracranial variables, should be evaluated thanks to principal stresses and strains in order to evaluate their ability to predict TBI.

Moreover, a special attention must be paid to the brain/skull interface modelling, since it influences significantly the brain dynamic response in terms of brain Von Mises stress for example. Thus, a modal analysis of the rat's head could be undertaken to identify its frequency response and its deformation mode shapes. Such a study would also allow establishing the elastic properties of the brain/skull interface as it has already been done for the human and for other inert structures like protective helmets by Willinger and al. (1990, 2000).

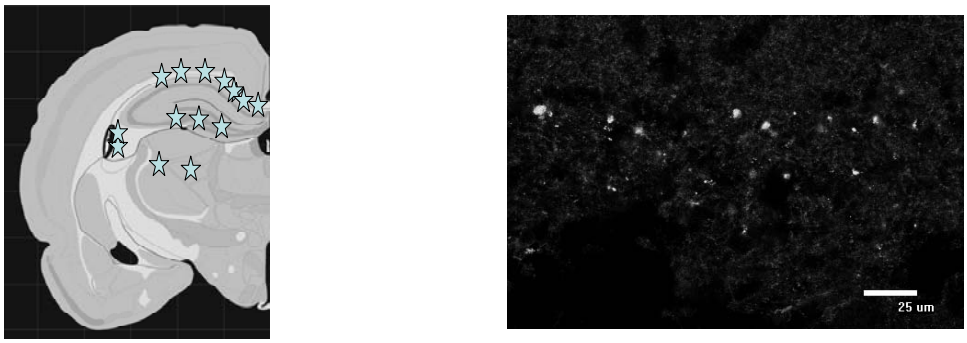


**Fig. 13 – Left: Stars indicating localization of β-APP-positive axons in schematics of the middle coronal section of the rat brain. Right: Confocal image of an example frontal section of the corpus callosum (upper part in image) and subcortical white matter (lower part of the image) incubated with β-APP (green) and NF-antibodies (red) indicating axonal injury.**

## LIMITATIONS OF THE STUDY

One of the main limitations of that study concerns the FEM of the rat's head itself. More precisely, the accuracy on the knowledge of the mechanical behavior of each anatomical component modeled is a critical question. Indeed, a great deal of previous studies showed the sensitivity of brain response to material properties and boundary conditions: Kleiven et al. (2006), Shafieian et al. (2007), Darvish et al. (2001, 2002), Anderson et al. (1999, 2003) or Wittek et al. (2003). In that field, the range of experimental data that are available varies extremely, and sometimes in a scale of more than thousand, shall it be for the brain viscous elastic characteristics or for the skull rupture properties. Obviously, the outcomes of the present work are highly dependent on these data. It was precisely the goal of the here presented parametric study to identify which mechanical parameter has to be known with high accuracy and which could be approximated more roughly. Nevertheless, efforts in the framework of further work are expected to build models that are increasingly efficient and biofidelic.

One other main limitation of that study relies on the validation data with regard to the experimental studies. The only common thing was the head acceleration input and the injury outcome. A complete validation of the model is made difficult by the limited availability of experimental validation data to confront the model with, such a brain pressure or displacement for example. Nevertheless, such a more accurate validation work is under

consideration for further steps. Indeed, high speed x-ray and some neutral density markers in planted in the brain tissue could allow measuring brain motions as well as brain/skull relative motion. Such techniques could also allow measuring strains in the brain tissue and tuning the stiffness of the FEM of the rat brain.

Another concern is the pattern and location registration between the high stress locations in the model and the observed injuries. Some inaccuracies remain regarding the local pressure during trauma for the injured regions, and about the exact volume of β-APP positive tissue. These are possible to estimate but need better software and procedures than the ones that are currently available in the authors' department. In despite of the level of this injury description, the model may evolve into being fitted with ventricles and possible different density and stiffness of the gray matter, as well as softer central regions compared to the cortex. Thus, brain mechanical field parameters could be calculated with greater accuracy.

## CONCLUSION

The current paper proposes an approach that relies on a combination of animal experimental testing and numerical modelling, in order to better understand TBI. The benefit relies in the well-defined external mechanical loading conditions of the head that usually lack in a "human approach" compared to an "animal approach". Moreover, a great number of impacts can be achieved, thus allowing a statistical analysis of the correlation between observed injuries and calculated intracranial mechanical parameters. Nevertheless, this FEM approach, mainly through the mechanical behaviour of its anatomical components, remains difficult to validate against experimental data because of the lack of such data. Therefore, efforts must continue in the identification of tissues properties of the small animal. Thus, innovating techniques, such as FEM, will offer the possibility to improve TBI identification.

## REFERENCES


Adelson P.D., Robichaud P., Hamilton R.L., Kochanek P.M., A model of diffuse traumatic brain injury in the immature rat, Journal of Neurosurgery, Vol. 85, pp. 877-884, 1996.

Adelson P.D., Jenkins L.W., Hamilton R.L., Robichaud P., Tran M.P., Kochanek P.M., Histopathologic response of the immature rat to diffuse traumatic brain injury, Journal of Neurotrauma, Vol. 18, N° 10, pp. 967-976, 2001.

Anderson R.W.G., Brown C.J., Blumbergs P.C., Scott G., Finnie J.W., Jones N.R., McLean A.J., Mechanisms of axonal injury: an experimental and numerical study of a sheep model of head impact, Proceedings of the 1999 IRCOBI Conference, pp. 107-120, 1999.

Anderson R.W.G., Brown C.J., Blumbergs P.C., McLean A.J., Jones N.R., Impact mechanics and axonal injury in a sheep model, Journal of Neurotrauma, Vol. 20, N° 10, pp. 961-974, 2003.

Baumgartner D., Willinger R., Human head tolerance limits to specific injury mechanisms inferred from real world accident numerical reconstruction, Revue Europeenne des Elements Finis, Vol. 14, N° 4-5, pp. 421-444, 2004.

Darvish K.K., Crandall J.R., Nonlinear viscoelastic effects in oscillatory shear deformation of brain tissues, Medical Engineering and Physics, Vol. 23, pp. 633-645, 2001.

Darvish K.K., Crandall J.R., Influence of brain material properties and boundary conditions on brain response during dynamic loading, Proceedings of the 2002 IRCOBI Conference, pp. 339-350, 2002.

Davidsson J., Risling M., Angeria M., A new model and injury threshold for sagittal plane rotational induced diffuse axonal injuries in the brain, Proceedings of the 2009 IRCOBI Conference, 2009.

Ellingson B.M., Fijalkowski R.J., Pintar F.A., Yoganandan N., Gennarelli T.A., New mechanism for inducing closed head injury in the rat, Biomedical sciences instrumentation, Vol. 41, pp. 86-91, 2005.

Fijalkowski R.J., Stemper B.D., Ellingson B.M., Yoganandan N., Pintar F.A., Gennarelli T.A., Inducing mild traumatic brain injury in the rodent through coronal plane angular acceleration, Proceedings of the 2006 IRCOBI Conference, pp.115-126, 2006.

Fijalkowski R.J., Stemper B.D., Pintar F.A., Yoganandan N., Crowe M.J., Gennarelli T.A., New rat model for diffuse brain injury using coronal plane angular acceleration, Journal of Neurotrauma, Vol. 24, N° 8, pp.1387-1398, 2007.

Foda M.A.A., Marmarou A., A new model of diffuse brain injury in rats. Part II: Morphological characterization, Journal of Neurosurgery, Vol. 80, pp. 301-313, 1994.

Gefen A., Gefen N., Zhu Q., Raghupathi R., Margulies S.S., Age-dependent changes in material properties of the brain and braincase of the rat, Journal of Neurotrauma, Vol. 20, N° 11, pp. 1163-1172, 2003.

Gutierrez E., Huang Y., Haglid K., Bao F., Hansson H.A., Hamberger A. et Viano D., A new model for diffuse brain injury by rotational acceleration: I model, gross appearance, and astrocytosis, Journal of Neurotrauma, Vol. 18, pp. 247-257, 2001.

Kallakuri S., Cavanaugh J.M., Cuneyt Ozaktay A., Takebayashi T., The effect of varying impact energy on diffuse axonal injury in the rat brain: a preliminary study, Experimental Brain Research, Vol. 148, N° 4, pp. 419-424, 2003.

Kleiven S., Evaluation of head injury criteria using finite element model validated against experiments on localized brain motion, intracerebral acceleration, and intracranial pressure, International Journal of Crashworthiness, Vol. 11, N° 1, pp. 65-79, 2006.

Krave U., Hojer S., Hansson H.A., Transient, powerful pressures are generated in the brain by a rotational acceleration impulse to the head, European Journal of Neuroscience, Vol. 21, pp. 2876-2882, 2005.

Levchakov A., Linder-Ganz E., Raghupathi R., Margulies S.S., Gefen A., Computational studies of strain exposures in neonate and mature rat brains during closed head impact, Journal of Neurotrauma, Vol. 23, N° 10, pp.1570-1580, 2006.

Mao H., Zhang L., Yang K.H., King A.I., Application of a finite element model of the brain to study traumatic brain injury mechanisms in the rat, Stapp Car Crash Journal, Vol. 50, pp. 583-600, 2006.

Mao H., Zhang L., Yang K.H., King A.I., Pal J., Gallyas F., Finite element analysis of a close head axonal injury model – Relating brain tissue biomechanics to skull deformation, Proceedings of the 2008 ASME Summer Bioengineering Conference, 2008.

Margulies S.S., Gefen A., Are in vivo and in situ brain tissues mechanically similar ?, Journal of Biomechanics, Vol. 37, N° 9, pp. 1339-1352, 2004.

Marjoux D., Baumgartner D., Deck C., Willinger R., Head injury prediction capability of HIC, HIP, SiMon and ULP criteria, Accident Analysis and Prevention, Vol. 40, N° 3, pp. 1135-1148, 2008.

Marmarou A., Foda M.A.A., van den Brink W., Campbell J., Kita H., Demetriadou K., A new model of diffuse brain injury in rats. Part I: Pathophysiology and biomechanics, Journal of Neurosurgery, Vol. 80, pp. 291-300, 1994.

Shafieian M., Darvish K., Effect of TBI on material properties of rat brain tissue**,** Proceedings of the 2007 IEEE Bioengineering Conference, pp. 283-284, 2007.

Ward C.C., Chan M., Nahum A.M., Intracranial pressure: a brain injury criterion, Proceedings of the 24th STAPP Car Crash Conference, SAE Paper n° 801304, 1980.

Willinger R, Cesari D, Evidence of cerebral movement at impact through mechanical impedance methods, Proceedings of 1990 IRCOBI Conference, pp. 203-213, 1990.

Willinger R., Baumgartner D., Guimberteau T., Dynamic characterization of motorcycle helmets: modelling and coupling with the human head, Journal of Sound and Vibration, Vol. 235, N° 4, pp. 611-625, 2000.

Wittek A., Omori K., Parametric study of effects of brain/skull boundary conditions and brain material properties on responses of simplified finite element model under angular acceleration impulse in sagittal plane, JSME International Journal, Vol. 46, N° C, pp. 1388-1399, 2003

Xiao-Sheng H., Sheng-Yu Y., Xiang Z., Zhou F., Jian-Ning Z., Li-Sun Y., Diffuse axonal injury due to lateral head rotation in a rat model, Journal of Neurosurgery, Vol. 93, pp. 626-633, 2000.

Zhang L., Yang K.H., Dwarampudi R., Omori K., Li T., Chang K., Hardy W.N., Khalil T.B., King A.I., Recent advances in brain injury research: a new human head model development and validation, Proceedings of the 45th STAPP Car Crash Conference, Vol. 45, 2001.